

**EFFECT OF GRAPHITE AND NbC ON MECHANICAL
PROPERTIES OF AISI304 BINDED WC**

TRAN BAO TRUNG

UNIVERSITI SAINS MALAYSIA

2013

**EFFECT OF GRAPHITE AND NbC ON MECHANICAL
PROPERTIES OF AISI304 BINDED WC**

by

TRAN BAO TRUNG

**Thesis submitted in fulfilment of the
requirements for the degree
of Doctor of Philosophy**

May 2013

ACKNOWLEDGEMENTS

I would like to express my most sincere thanks that come deeply from my heart to those who in one way or another contributed to make this research study possible.

Firstly, I am deeply grateful to my main supervisor, Assoc. Prof. Dr. Zuhailawati Hussain for her supervision and advice from the early to the final stage of this research work. She has always been patient and encouraging in times of new ideas and difficulties. She has listened to my ideas and discussed frequently with me which led to the key insights of my work. She is a true scientist and a dedicated teacher that I want to be. Above all, she made me feel a friend, which I appreciate from my heart.

I would like to express my sincere gratitude to my co-supervisor Prof. Zainal Arifin Ahmad for his helps in all the time of this research. I have never forgotten his supports, for his patience, motivation, enthusiasm, and immense knowledge. He is a great teacher that I have met. I keep in my mind his impressive saying to me “Take a seat and talk to me as a friend”.

I would like to deliver my thanks to my Japanese advisor Prof. Ishihara N. Keiichi, the School of Energy Science, Kyoto University, for his guidance and advice on my research. Special thanks to Prof. Hideyuki Okumura and Dr. Eiji Yamasue for their supports during the time of my study in Japan.

I am grateful to Professor Dr. Hanafi Ismail as the Dean and the staffs of the School of Materials and Mineral Resources Engineering, Universiti Sains Malaysia, for their kindness and support.

This work would not have been possible without the financial support and cares from AUN-SEED Net/JICA. I would like to deliver my sincere thanks and

deepest gratitude for their generosity in giving me this opportunity to pursue my Ph.D.'s degree.

My special thanks and appreciation are also extended to those people who, in one way or another, helped me accomplish this research:

To Mdm. Fong, Mr. Kemuridan, Mr. Shahid, Mr. Farid, Mr. Khairi, Mr. Rashid, Mr. Zaini, Mr. Fadzil, and Mr. Fujimoto Shoji for their kindness, help, and assistance.

To all my friends: Duong, Long, Bang, Viet, Mahani, Anny, Nini, Sunisa, Zahir, Macara, Endo, Siba, Luong, Luyen, etc.

Last but not the least, I would like to take this opportunity to express my gratitude to my family for their love.

Thank you to all of you!

TABLE OF CONTENTS

	Page
ACKNOWLEDGEMENTS	ii
TABLE OF CONTENTS	iv
LIST OF TABLES	x
LIST OF FIGURES	xi
LIST OF ABBREVIATIONS	xvi
LIST OF SYMBOL	xvii
ABSTRAK	xviii
ABSTRACT	xix

CHAPTER 1: INTRODUCTION

1.1	Introduction	1
1.2	Problem statements	4
1.3	Objectives of study	6
1.4	Research scope	7

CHAPTER 2: LITERATURE REVIEW

2.1	History of tungsten carbide and hard metals	10
2.2	Binder phase	13
2.2.1	Cobalt binder	14
2.2.2	Nickel binder	16
2.2.3	Iron binder	18
2.2.4	Ni-Fe and Co-Ni-Fe binders	19

2.2.5	Fe-Cr-Ni binders and stainless steel binder	20
2.3	η - Phase	21
2.4	Graphite	24
2.5	Consolidation tungsten carbide hard metal powders	25
2.5.1	Green consolidation	25
2.5.2	Sintering process	27
2.5.2.1	Solid state sintering	27
2.5.2.2	Liquid phase sintering (LPS)	33
2.5.3	Grain growth	36
2.5.4	Grain growth inhibitors	38
2.6	Sintering method	42
2.6.1	Vacuum sintering	43
2.6.2	Hot pressing	43
2.6.3	Hot isostatic pressing	44
2.6.4	Pseudo hot isostatic pressing	44
2.7	Mechanical properties of WC-hard metals	45
2.7.1	Hardness of WC-hardmetals	46
2.7.2	Fracture toughness of WC-hardmetals	49
2.7.3	Other mechanical properties of WC-based hardmetals	52
2.8	Mechanical alloying	53
2.8.1	Introduction of mechanical alloying	54
2.8.2	Mechanical alloying mechanisms	55
2.9	Summary	57

CHAPTER 3: RAW MATERIALS AND METHODOLOGY

3.1	Raw Materials	59
3.1.1	Tungsten carbide (WC) powder	59
3.1.2	Stainless steel powder	60
3.1.3	Niobium carbide (NbC) powder	60
3.1.4	Graphite powder	61
3.2	Research methodology	61
3.2.1	Mixing of WC-FeCrNi hardmetal powders by planetary ball milling	63
3.2.2	Green body compaction	64
3.2.3	Sintering in a vacuum furnace	64
3.2.4	Sintering by PHIP process	65
3.3	Data analysis	67
3.3.1	Phase identification	67
3.3.2	Microstructure observation	68
3.3.3	Density measurement	69
3.3.4	Hardness testing	70
3.3.5	Fracture toughness measurement	71

CHAPTER 4: RESULTS AND DISCUSSION

4.1	Raw material analysis	73
4.1.1	Tungsten carbide (WC) powder	73
4.1.2	FeCrNi powder	74
4.1.3	Graphite (C _{gr}) powder	76

4.1.4	Niobium carbide (NbC) powder	78
4.2	Effect of milling time on microstructure and mechanical properties of WC-10FeCrNi hardmetals	79
4.2.1	Phase identification and microstructure of as-milled powder	80
4.2.2	Phase identification and microstructure of sintered samples	83
4.2.3	Density measurement	87
4.2.4	Hardness and fracture toughness	88
4.3	Effect of sintering temperature on microstructure and mechanical properties of WC-10FeCrNi hardmetals	90
4.3.1	Phase identification and microstructure of sintered samples	90
4.3.2	Density measurement of sintered samples	93
4.3.3	Hardness and fracture toughness	95
4.4	Effect of sintering time on the microstructure and mechanical properties of WC-10FeCrNi hardmetals	96
4.4.1	Phase identification and microstructure of sintered samples	96
4.4.2	Density of sintered samples	101
4.4.3	Mechanical properties of sintered samples	102
4.5	Role of binder phase composition	103
4.5.1	The role of binder in phase and microstructure of sintered samples	104
4.5.2	Density of sintered samples	107
4.5.3	Hardness and fracture toughness of sintered samples	107
4.6	Effect of graphite addition on microstructure and mechanical properties WC-10FeCrNi hardmetals	109

4.6.1	Phase identification and microstructures	109
4.6.2	Density of sintered samples	113
4.6.3	Vickers hardness and fracture toughness	115
4.6.4	Summary	116
4.7	Role of NbC addition on vacuum sintered WC-10FeCrNi-2C _{gr} hardmetals	117
4.7.1	Phase identification and microstructures	117
4.7.2	Density of sintered samples	122
4.7.3	Hardness and fracture toughness	123
4.7.4	Summary	124
4.8	The role of NbC addition as WC grain growth inhibitor for PHIP sintered WC-10FeCrNi-2graphite hardmetals	125
4.8.1	Phase identification and microstructure	125
4.8.2	Density measurement	132
4.8.3	Hardness and fracture toughness	132
4.8.4	Summary	136
4.9	Effect of temperature on microstructure and mechanical properties of samples sintered by PHIP	137
4.9.1	Phase identification and microstructure	137
4.9.2	Density measurement	141
4.9.3	Hardness and fracture toughness of sintered samples	142
4.9.4	Summary	143
4.10	Effect of pressure on the microstructure and mechanical properties of PHIP sintered samples	144
4.10.1	Phase identification and microstructure	144

4.10.2	Density measurement	147
4.10.3	Hardness and fracture toughness	148
4.10.4	Summary	149

CHAPTER 5: CONCLUSION AND RECOMMENDATIONS

5.1	Conclusion	150
5.2	Recommendations	152

REFERENCES	153
-------------------	------------

APPENDIX	174
-----------------	------------

LIST OF TABLES

		Page
Table 2.1	Physical and mechanical properties of some WC-Co hardmetals	15
Table 2.2	Characteristic stages of liquid phase sintering	35
Table 2.3	The relationship between hardness and microstructural parameters	48
Table 2.4	Expressions for fracture toughness (K _{IC}) calculation from Vickers indentation crack systems	52
Table 3.1	Physical properties of WC	59
Table 3.2	Properties of alloy AISI304	60
Table 3.3	Physical properties of niobium	61
Table 3.4	Physical properties of graphite	61
Table 4.1	η -phase fraction formed with vs. sintering temperatures	92
Table 4.2	Composition of samples	104
Table 4.3	Composition of samples with graphite addition	109
Table 4.4	Composition of sample with NbC addition	117
Table 4.5	WC grain size of vacuum sintered samples with NbC addition	122
Table 4.6	Composition of sample with NbC addition sintered by PHIP	125
Table 4.7	Amount of η -phase of PHIP-sintered samples various with NbC contents	129
Table 4.8	WC grain size of PHIP sintered samples with NbC addition	131
Table 4.9	Relative densities of sintered samples	132

LIST OF FIGURES

		Page
Fig. 2.1	W-C phase diagram	10
Fig. 2.2	The atomic structure of WC crystal	11
Fig. 2.3	Vertical section of W-C-Co calculated at 10 wt.% Co	15
Fig. 2.4	Vertical section of W-C-Ni calculated at 10 wt.% Ni	18
Fig. 2.5	Vertical section of W-C-Ni calculated at 10 wt.% Fe	19
Fig. 2.6	Figure 2.6 W-Co-C isothermal sections: a) at 1000°C and b) 1400°C	23
Fig. 2.7	Crystal structure of Fe ₃ W ₃ C	24
Fig. 2.8	Crystal of α -graphite	25
Fig. 2.9	Compressibility curves of the ball milled WC-10Co powders	26
Fig. 2.10	Stages of densification of a range of WC-Co alloys; Stage I below eutectic temperature; Stage II densification at eutectic temperature and Stage III subsequent densification	28
Fig. 2.11	SEM images of morphology evolution of WC-10Co_10 nm powders when heated at different temperatures: (a) as-milled powder, (b) 800°C, (c) 1000°C, (d) 1100°C (e) 1200°C, and (f) 1300°C	30
Fig. 2.12	Schematic representation of WC particles bounded by the Co binder phase	31
Fig. 2.13	Schematic of the hardmetal solid state sintering mechanism (a, b, c, d, e) (Silva et al., 2001) and (f) Cobalt spreading on WC plate at 1050°C under argon, 1-WC, 2-WC/Co region and 3-Co particle	33
Fig. 2.14	SEM images of a) WC-30Co and b) WC-30Co-1VC sintered at 1400°C for 1h in a vacuum furnace	40
Fig. 2.15	The relationship between Vickers hardness and volume percent Co	47
Fig. 2.16	(a) The correlation of the fracture toughness K_{IC} with the mean linear path in binder phase λ , and (b) with the carbide crystals contiguity G	49
Fig. 2.17	The correlation between hardness and fracture toughness of WC-Co and with added cubic carbides	50

Fig. 2.18	Schematic of Vickers indentation cracks and Palmqvist cracks: d- diagonal of the indentation left in the surface; l- Palmqvist crack length	51
Fig. 2.19	Ball-powder-ball collision of powder mixture during mechanical alloying	56
Fig. 3.1	Flow chart of the experimental procedure	62
Fig. 3.2	Sintering diagram of samples in the vacuum furnace	65
Fig. 3.3	Heating diagram of PHIP process	66
Fig. 3.4	Schematic diagram of experiment set up for PHIP. (1) Die, (2) Heating coil, (3) Specimen, (4) Upper punch, (5) Lower punch, (6) Thermocouple, (7) Electric circuit, and (8) Silica sand powder	66
Fig. 3.5	PHIP system and sample fabrication process: 1 – Heating coil, 2 – Sample, 3 – Stainless steel mould, 4 – Silica sand, 5 – Thermocouple, 6 – Upper punch, 7 – Putting in pressing chamber and connecting with pressing system, 8 – Pressure gauge, 9 – Pressing chamber, 10 – System controlling	67
Fig. 3.6	Schematic of indentation mark in Vickers hardness measurement	71
Fig. 3.7	FESEM image of indentation on sample WC-10FeCrNi-2C _{gr} -1NbC sintered by PHIP at 1300°C for 45 min including 15 min pressing at 20 MPa and the crack lengths at the corners of the indentation (L1-L4)	72
Fig. 4.1	XRD patterns of WC raw powders	73
Fig. 4.2	a) FESEM image and b) EDX result of WC raw powder	74
Fig. 4.3	XRD patterns of FeCrNi powders	75
Fig. 4.4	a) FESEM image and b) EDX result of FeCrNi powders	76
Fig. 4.5	XRD patterns of graphite powders	77
Fig. 4.6	a) FESEM image and b) EDX result of C _{gr} powders	77
Fig. 4.7	XRD patterns of NbC powders	78
Fig. 4.8	a) SEM image and b) EDX result of NbC powders	79
Fig. 4.9	XRD patterns of WC-10FeCrNi powders at different milling time	80
Fig. 4.10	WC crystallite size at different milling time	82
Fig. 4.11	Back scattered electron FESEM images of WC-10FeCrNi at various milling time: a) 5 h, b) 10 h, c) 15 h and d) 20 h	83
Fig. 4.12	a) XRD patterns of sintered samples at 1300°C and b) magnification at 40-50 of 2θ degree	84

Fig. 4.13	η -phase fraction vs. milling time of sintered samples at 1300°C	85
Fig. 4.14	Back scattered electron FESEM images of sintered samples at different milling time; arrows show the pores in the microstructures	87
Fig. 4.15	Relative densities of pre-compacted and sintered samples at 1300°C	88
Fig. 4.16	Vickers hardness and fracture toughness vs. milling time	89
Fig. 4.17	a) XRD patterns of sintered WC-10FeCrNi at different temperatures and b) magnification at 35-55 of 2θ	81
Fig. 4.18	FESEM back scattered electron images of sintered WC-10FeCrNi at different temperatures:a) 1250°C, b)1300°C, d) 1350°C for 1 h and EDX result of point X in Fig. 4.18a	93
Fig. 4.19	Relative density of WC-FeCrNi at different sintering temperature	94
Fig. 4.20	Vicker hardness and fracture toughness of sintered samples vs. sintering temperatures	96
Fig. 4.21	a) XRD patterns of sintered samples at different sintering time; 15, 30, 45 and 60 min, and b) magnification at 35-55degree of 2θ	97
Fig. 4.22	η -phase fraction various with sintering time	98
Fig. 4.23	Back scattered electron images of sintered WC-10FeCrNi at different sintering time: a, 15min; b) 30min; c) 45min and d) 60min, and EDX analysis of X, Y, Z and W points in SEM images	100
Fig. 4.24	Effect of sintering time on the density of sintered sample	101
Fig. 4.25	Vickers hardness and fracture toughness of samples at various sintering time	103
Fig. 4.26	XRD patterns of samples various with binder content sintered at 1350°C	105
Fig. 4.27	η -phase fraction vs. initial binder contents	105
Fig. 4.28	SEM back-scatter electron images of samples sintered at 1350°C with different binder contents	106
Fig. 4.29	Density and relative density of samples vs. initial binder contents	107
Fig. 4.30	Vickers hardness and fracture toughness of sintered samples with different binder content	108
Fig. 4.31	XRD patterns of mixed powders with graphite addition	110
Fig. 4.32	XRD patterns of sintered samples vs. graphite addition	111
Fig. 4.33	FESEM backscattered electron images of samples after sintering at	113

	1350°C in vacuum furnace various with graphite contents: 0 wt.% HC0, 1 wt.% HC1, 1.5 wt.% HC2, 2 wt.% HC3, 2.5wt.% HC4, 3 wt.% HC5	
Fig. 4.34	Relative densities of sintered samples vs. graphite contents	114
Fig. 4.35	Vickers hardness, HV30, and fracture toughness of sintered samples	116
Fig. 4.36	a) XRD patterns of milled samples various with NbC contents and b) magnification at 40-50 of 2θ	118
Fig. 4.37	XRD patterns of vacuum sintered samples with vs. NbC contents	119
Fig. 4.38	Figure 4.38 FESEM back scattered electron images of sintered samples with different NbC contents	120
Fig. 4.39	EDX result of point X in Fig. 4.30 (HN5)	122
Fig. 4.40	Density of sintered sample vs. NbC content	123
Fig. 4.41	Vickers hardness of as-sintered samples with NbC addition	124
Fig. 4.42	XRD patterns of samples HS1 and HS6 after sintering	126
Fig. 4.43	FESEM back-scattered electron images of as-sintered samples: (a) HS1 and (b) HS6	127
Fig. 4.44	XRD patterns of as-sintered samples with various amounts of NbC; 0 wt.% NbC (HS1), 1 wt.% NbC (HS2), 1.5 wt.% NbC (HS3), 2 wt.% NbC (HS4) and 5 wt.% NbC (HS5)	129
Fig. 4.45	FESEM back-scattered images of as-sintered samples with: (a) 1 wt.% NbC (HS2), (b) 1.5 wt.% NbC (HS3), (c) 2 wt.% NbC (HS4) and (d) 5 wt.% NbC (HS5)	130
Fig. 4.46	EDX analysis of a) point X in Fig. 4.45c and b) point Y in Fig. 4.45d	131
Fig. 4.47	Hardness and fracture toughness of PHIP-sintered samples vs with NbC addition	133
Fig. 4.48	(a)-Hardness and (b)-fracture toughness of this work compared with references	135
Fig. 4.49	XRD patterns of WC/10FeCrNi-1NbC sintered by PHIP at different temperature	138
Fig. 4.50	FESEM back-scattered images of PHIPed-samples at: (a) 1150°C, (b) 1200°C, (c) 1250°C and (d) 1300°C	139
Fig. 4.51	Density of PHIPed samples at different temperature	141
Fig. 4.52	(a) Vickers hardness and (b) fracture toughness of WC-10FeCrNi-2graphite-1NbC sintered by HIP and WC-10FeCrNi sintered in vacuum furnace	142

Fig. 4.53	XRD patterns of PHIPed samples vs. applied pressure	144
Fig. 4.54	η -phase fraction vs. applied pressure in PHIP process	145
Fig. 4.55	FESEM back scattered electron images of samples vs. pressure in PHIP	146
Fig. 4.56	Density vs. applied pressure of samples sintered by PHIP	147
Fig. 4.57	Hardness and fracture toughness vs. pressure of PHIPed samples	148

LIST OF ABBREVIATIONS

Ar	Argon gas
bcc	Body centered cubic
BPR	Ball to powder ratio
EDX	Energy dispersion X-ray spectroscopy
fcc	Face centered cubic
FESEM	Field emission scanning electron microscopy
FeCrNi	AISI304 stainless steel
hcp	Hexagonal closed pack
HIP	Hot isostatic pressing
LPS	Liquid phase sintering
MA	Mechanical alloying
PHIP	Pseudo hot isostatic pressing
rpm	Rotation per minute
TRS	Transverse rupture strength
XRD	X-ray diffraction

LIST OF SYMBOLS

$\dot{\epsilon}$	Shrinkage rate
ϵ	Plastic strain
α	Ferrite structure
γ	Austenite structure
σ	Yield strength
ρ	Density
Ω	Average atomic volume
C	Contiguity
d	Half diagonal indentation
D	Grain size
E	Young's Modulus
H	Hardness
HV	Vickers hardness
K_{IC}	Fracture toughness
L	Palmqvist crack length
$\langle x \rangle$	Mean radius

ABSTRAK

Kajian ini mengkaji peranan keluli nirkarat AISI304 untuk menggantikan Co sebagai bahan pengikat untuk logam keras berasaskan WC. Serbuk WC-AISI304 dihasilkan dari serbuk bahan mentah (WC dan AISI304) menggunakan kaedah pengalioian mekanikal. Serbuk logam keras kemudiannya disinter menggunakan dua kaedah pensinteran; pensinteran vakum dan pensinteran PHIP. Untuk memperbaiki sifat-sifat mekanikal sampel tersinter, grafit (C_{gr}) dan NbC telah ditambahkan sebelum pengisaran. Keputusan menunjukkan bahawa fasa- η (Fe_3W_3C) terbentuk di dalam sampel-sampel tersinter ketika proses pensinteran. Penambahan C_{gr} telah mengurangkan pembentukan fasa- η . Disebabkan fasa ini dihapuskan, kedua-dua kekerasan dan kekuatan patah sampel tersinter telah meningkat. Tumbesaran butir WC boleh direncatkan dengan penambahan NbC. Peningkatan kandungan NbC menyebabkan peningkatan kekerasan tetapi mengurangkan kekuatan patah sampel tersinter. Di samping itu, kajian ini juga menunjukkan potensi yang tinggi PHIP dalam menjanakan ketumpatan sampel yang lebih tinggi berbanding pensinteran vakum. Oleh itu, kaedah ini boleh meningkatkan sifat-sifat mekanikal logam keras WC-AISI304. Kekerasan Vickers logam keras WC-AISI304- $2C_{gr}$ - $xNbC$ ($x = 1 - 5$) yang dihasilkan ialah dalam julat 1600 ke 1660 kg/mm^2 dan kekuatan patah, K_{IC} , dari 8.7 ke 8.3 $MPa.m^{1/2}$ apabila menggunakan pensinteran vakum. Walau bagaimanapun, sampel yang sama yang dihasilkan melalui pensinteran PHIP memberikan kekerasan Vickers dari 1640 ke 1820 kg/mm^2 dan kekuatan patah, K_{IC} , dari 10 ke 7.3 $MPa.m^{1/2}$. Nilai-nilai kekerasan dan kekuatan patah ini adalah dalam julat pertengahan berbanding dengan sistem yang disebutkan dalam tinjauan persuratan. Keputusan ini menunjukkan bahawa AISI304 boleh dicadangkan untuk menggantikan bahan pengikat dari Co sebagai usaha untuk menghasilkan alat pemotong.

ABSTRACT

This work studies the role of AISI304 stainless steel as a Co replacement binder for WC-based hardmetals. WC-AISI304 hardmetal powders were produced from raw powders (WC and AISI304) by mechanical alloying technique. The hardmetal powders were then sintered by two sintering methods; vacuum sintering and PHIP sintering. To improve mechanical properties of sintered samples, graphite (C_{gr}) and NbC were added prior to milling. The results show that η -phase (Fe_3W_3C) formed in the sintered samples during sintering. C_{gr} addition has enabled to reduce the formation of η -phase. As this phase was eliminated, both hardness and fracture toughness of sintered sample were improved. WC grain growth can be inhibited by the addition of NbC. Increasing NbC content led to an increase of hardness but reduce fracture toughness of sintered samples. Besides that, this work also show a higher potential of PHIP in generating higher density of sintered samples compared to vacuum sintering, and hence, improving mechanical properties of WC-AISI304 hardmetals. The Vickers hardness of WC-10AISI304-2 C_{gr} -xNbC ($x = 1 - 5$) hardmetals produced is in range of 1600 to 1660 kg/mm^2 and fracture toughness, K_{IC} , from 8.7 to 8.3 $MPa.m^{1/2}$ by vacuum sintering. However, the same samples produced via PHIP sintering gave the Vickers hardness from 1640 to 1820 kg/mm^2 and fracture toughness, K_{IC} , from 10 to 7.3 $MPa.m^{1/2}$. These values of hardness and fracture toughness are in the intermediate range compared to other systems provided by literatures. The results indicate that AISI304 could be proposed to replace Co binder in order to fabricate cutting inserts.

CHAPTER 1

INTRODUCTION

1.1 Introduction

WC-based hardmetals have been developed since 1920s and widely used in cutting tool industries. The combination between the high hardness of WC particles and high ductility of the binders (Co, Ni or Fe) produces a hardmetal with high hardness, high fracture toughness and good wear resistance. These properties are very important in industries such as cutting edges in turning machines, drilling screws in mining equipments, and die industries and so on (Jorn, 1985; Ettmayer, 1989; Hanyaloglu et al., 2001; Fernandes and Senos, 2011). WC-based carbide hardmetals dominate about 95% of cemented carbide cutting tools in the market (Yao et al., 1999). The annual report of W for use in WC worldwide shows that in 2008, 50,000 tons of W were consumed which account for nearly 60% of the world's W consumption including recycled materials (Schubert et al., 2010).

In recent decades, many researches have been carried out to improve the mechanical properties of WC-Co hardmetals by controlling their microstructures. Fine and ultrafine grained WC hardmetals are more important today for high performance of cutting tools, chipless formation or other applications. As a rule, the importance of finer grain size of WC is derived from the understanding that hardness and wear resistance increase with decreasing WC grain size (Kim et al., 1997; Niels, 2004; Huang et al., 2008b). However, sintering WC-Co process is often performed at temperatures ranging from 1300-1500°C in a vacuum furnace, thus grain growth of WC takes place and consequently, the mechanical strength and hardness of the tools are limited.

Mechanical alloying or other synthesis methods could be used to gain nano particles or ultrafine WC powders effectively but abnormal grain growth could occur and affect the mechanical properties of hardmetals. In this case, a small amount of some other carbides such as VC, NbC, TiC, TaC or Cr₂C₃ have been added to work as the grain growth inhibitors during sintering process (Huang et al., 2007; Huang et al., 2008a; Huang et al., 2008b; Barbatti et al., 2009; Mahmoodan et al., 2009; Weidow et al., 2009a). The advance sintering methods to limit WC grain growth have been investigated using a variety of techniques including liquid phase sintering, hot isostatic pressing (HIP) (Soares et al., 2012), spark plasma sintering (SPS) (Zhang et al., 2004b; Sivaprahasam et al., 2007), microwave sintering (Breval et al., 2005), high frequency induction-heated and pulse plasma sintering (Kim et al., 2004; Kim et al., 2007; Shon et al., 2009).

Since the first patent of WC-based hardmetals was issued around 1923 by Schröter in the German company "Osram Studiengesellschaft", Co is the best choice as the binder of WC-based hardmetals (Schroter, 1925). WC-Co hardmetals have excellent mechanical properties such as high hardness, high strength and fracture toughness, and high wear resistance (Viswanadham and Lindquist, 1987; Ettmayer, 1989; Hanyaloglu et al., 2001; Weidow et al., 2009a; Schubert et al., 2010). However, recently, there are an increasing suspects of work diseases concerning with Co and WC-Co containing dust. Several reports have shown that occupational exposure to Co-containing dust has been associated with the development of different pulmonary diseases including fibrosing alveolitis and lung cancer (David et al., 1990; Lison et al., 1995; De Boeck et al., 2003; Koutsospyros et al., 2006). The excessive chronic inhalation of hardmetal particles can be associated with the occurrence of different lung diseases including an excess of lung cancers. The elective toxicity of hardmetals

is based on a physico-chemical interaction between Co metal and WC particles to produce activated oxygen species resulting in induction of DNA damage (De Boeck et al., 2003).

Besides that due to the high cost and depleting of Co, and the need to improve some properties of WC-based hardmetals such as corrosion resistance and oxidation resistance (Penrice, 1987; Gille et al., 2000; Fernandes and Senos, 2011), many studies have been carried out to find new binders to replace Co in WC-based hardmetals. Some transition metals have been investigated to replace Co with other elements such as Ni, Fe, Cr and Mn and show that it is possible to obtain high density after sintering at temperatures near to those used for WC/Co cemented carbides. The use of Ni binder has been shown to increase corrosion resistance of WC-based hardmetals compared to WC-Co (Tracey, 1992). The addition of Cr or Cr combined with Ni in the binder phase has been reported not only to improve oxidation and corrosion resistance but also to act as WC grain growth inhibitor in WC-based hardmetals (Penrice, 1987; Tracey, 1992).

The replacement of Fe-Mn alloys also make improvement in WC hardmetal properties such as hardness and toughness, however, the optimum composition has not been pointed out (Hanyaloglu et al., 2001). The development of Fe-Ni binders also can be seen in literature (Penrice, 1987; Uhrenius et al., 1997). Fe-rich alloys have been preferred as binders, not only because they are inexpensive but also because they improve mechanical properties and enhance sinterability due to their good wettability with WC (Uhrenius et al., 1997).

Recently, Fe rich alloys and stainless steel have been reported to have a potential to replace Co in WC based cemented carbides. One research team have

intensively used sputtering technique to coat WC powder with stainless steel and Fe rich alloys and discovered some advantages of these alloys to replace Co in densification (Fernandes et al., 2003b; Fernandes et al., 2007; Fernandes, 2008; Fernandes et al., 2009a; Fernandes et al., 2009b). They reported good sintering characteristics of the resultant composite powders and an improvement in the hardness of those hardmetals (Fernandes et al., 2003b; Fernandes et al., 2009b).

As known, AISI304 stainless steel is a basic grade of austenite stainless steel containing 18 wt.% of Cr and 8-10 wt.% of Ni. It possesses high strength, and high oxidation and corrosion resistance in comparison to plain carbon steel. The presence of Cr and Ni in this composition can combine their benefits in the binder phase for WC-based hardmetals (Penrice, 1987; Tracey, 1992; Uhrenius et al., 1997). Considering the potential of stainless steel as a binder replacement to Co, this research was carried out using AISI304 stainless steel to work as metal binder phase in WC-based hardmetal. This research investigated the role of binder phase in terms of binder content, sintering time, sintering temperature as well as sintering methods on the microstructure and mechanical properties of sintered samples such as hardness and fracture toughness. Beside that the effect of grain growth inhibitor and microstructure controlling by additional components such as NbC and graphite was also studied.

1.2 Problem statements

Literatures show a good sintering characteristic of WC/Fe-alloys or stainless steel hardmetals and good wetting properties of WC with iron-alloys. The reports show that liquid binder phase was formed at eutectic temperature about 1150°C for

WC-Fe rich binder phase (Fernandes et al., 2003b; Fernandes et al., 2007), which make this temperature suitable for liquid state sintering. However, similar to WC-Co system, the formation of η -phase $((M,W)_6C$, $M = \text{metal}$) has been reported during sintering of WC-Fe rich alloys hardmetals (Fernandes et al., 2003b; Fernandes et al., 2007; Fernandes et al., 2009a; Fernandes et al., 2009b). The formation of η -phase in the microstructure has been attributed to decarburization of WC during sintering or to a C content in the initial composition that is below the critical minimum necessary to prevent the formation of η -phase (Fernandes et al., 2007; Fernandes et al., 2009b). η -phase were reported to form during sintering WC coated with stainless steel at low temperature, of about 750°C and increases with temperature up to 1100°C (Fernandes et al., 2007). They also have reported that the η -phase, in the temperature ranging from 1200-1325°C, can be represented approximately as $(Fe_{2.3}Ni_{0.3})(Cr_{0.6}W_{2.8})C$. The presence of this brittle phase leads to a decrease in mechanical properties, particularly in fracture toughness (Uhrenius et al., 1997; Yao et al., 1998; Upadhyaya et al., 2001).

Thus, eliminating the formation of this phase becomes an important point in fabrication of WC-based hardmetals with new binders. It is reported that 2.5 -3 wt.% graphite has an ability to eliminate the formation of η -phase for sintering WC-10Fe rich alloys hardmetals (Fernandes et al., 2007; Fernandes et al., 2009a). So the role of graphite content addition on the microstructure and mechanical properties of the new WC-based hardmetals need clarification in particular its hardness and fracture toughness.

Although several researches have been reported on sintering WC/Fe-alloys or stainless steel binders (Hanyaloglu et al., 2001; Fernandes et al., 2003b; Fernandes et

al., 2007), the grain growth of WC in these kinds of binder phases is not well known. Controlling grain growth of WC in iron-alloys or stainless steel binders through the addition of grain growth inhibitor and the use of different sintering temperatures are necessary to be investigated. It is known that NbC has been used up to 5 wt.% as WC grain growth inhibitor for WC-Co system during sintering (Huang et al., 2008a). Thus, it is necessary to investigate the ability of NbC as the WC grain growth inhibitor in WC/Fe-alloy system.

In general, WC-based hardmetals could be sintered in a vacuum furnace which is sufficient for sintering large number of products and requirement equipments but the full densification is difficult to attain. In this case advanced sintering methods, including hot isostatic pressing (HIP) and spark plasma sintering (SPS), are the most suitable in order to achieve higher density of sintered samples. However, since the typical hot isostatic pressing is too expensive, low cost and simple isostatic pressing technique, such as pseudo hot isostatic pressing (PHIP) which uses sand as a pressure delivery medium, is proposed. Thus, an investigation on densification of WC in stainless steel binder during PHIP is required because information about this process is limited. PHIP is an advanced technique to produce high densification of sintered samples (Park et al., 1996; Xu et al., 2003; Zhang et al., 2010). Considering PHIP promises high mechanical properties of sintered samples, PHIP process was also used in comparison to vacuum sintering method to sinter the samples.

1.3 Research objectives

To solve the stated problem statements and in order to investigate the ability of stainless steel as a binder to WC-based hardmetals, this research aimed to fabricate

WC/AISI304-stainless steel hardmetals using different sintering methods (in a vacuum furnace and PHIP sintering) with improved mechanical properties

The objectives are listed as following:

1. To study the effect of milling time, sintering time, temperature and binder content on the microstructure and mechanical properties of WC/AISI304 hardmetals sintered in a vacuum furnace.
2. To control the formation of η -phase during vacuum sintering process by adding graphite in order to compensate C lost.
3. To investigate the ability of NbC to inhibit WC grain growth during sintering for mechanical properties improvement.
4. To study the effects of sintering temperature and pressure on the microstructure and mechanical properties of WC/AISI304 hardmetals sintered by PHIP.

1.4 Research scope

AISI304 stainless steel (namely as FeCrNi) was used as the binder in WC-based hardmetal. WC was mixed with FeCrNi powders by a planet ball milling to produce WC-AISI304 hardmetal powders. The effect of milling to produce high homogeneity of WC and FeCrNi powders and the role of binder phase was studied according to the following flow:

In order to optimization of milling process in term of milling time: WC-10FeCrNi (wt.%) powders were fabricated at different milling time (5, 10, 15 and 20h). The pre-compacted samples were sintered at 1300°C in a vacuum furnace

and then, investigated microstructure and mechanical properties (hardness and fracture toughness).

The effect of sintering temperature: WC-10FeCrNi (wt.%) powders milled at 15h were pre-compacted and sintered 1h at different temperature (1250, 1300 and 1350°C) in the vacuum furnace.

The role of sintering time: WC-10FeCrNi (wt.%) powders milled at 15h were pre-compacted and sintered at 1350°C under vacuum with different sintering time; 15, 30, 45 and 60 min.

The role of binder content: 8, 10, 12 and 15 wt.% of FeCrNi were mixed with WC by ball milling at 15h. The pre-compacted powders were then sintered at 1350°C for 1h in the vacuum furnace.

1, 1.5, 2, 2.5 and 3 wt.% of C_{gr} were added in WC-10FeCrNi before milling for 15h to eliminate the formation of η-phase during sintering at 1350°C for 1 h in the vacuum furnace.

1, 1.5, 2, 5 wt.% of NbC were added in WC-10FeCrNi-C_{gr} to investigate ability of NbC to inhibit WC grain growth during sintering at 1300°C for 1 h in the vacuum furnace.

To study the role of PHIP sintering method, 1, 1.5, 2, 5 wt.% of NbC were added in WC-10FeCrNi-C_{gr} to investigate ability of NbC to inhibit WC grain growth during sintering. PHIP was done at 1300°C for 45 min including 15 min pressing at 20 MPa, and as well as the effect of PHIP method on the microstructure and mechanical properties of WC-10FeCrNi hardmetals.

The effect of sintering temperature by PHIP: WC-10FeCrNi- C_{gr}-1NbC were sintered at 1200, 1250 and 1300°C for 45 min including 15 min pressing at 20 MPa.

The effect of loading pressure by PHIP: WC-10FeCrNi-C_{gr}-1NbC was sintered at 1300°C for 45 min including 15 min pressing at 0, 5, 15, 20 and 25 MPa.

CHAPTER 2

LITERATURE REVIEW

2.1 History of tungsten carbide and hard metals

The discovery of tungsten carbides was marked to the invention of W_2C in 1896 by Moissan, and of WC in 1898 by Williams, working at Moissan's laboratory at the school of Pharmacy at the University of Paris (Yao et al., 1998; Yao et al., 1999). Fig. 2.1 shows the advance W-rich part of the binary W-C equilibrium diagram (Kurlov and Gusev, 2006). Three stoichiometries have been found: β - W_2C , γ - WC_{1-x} , and δ -WC.

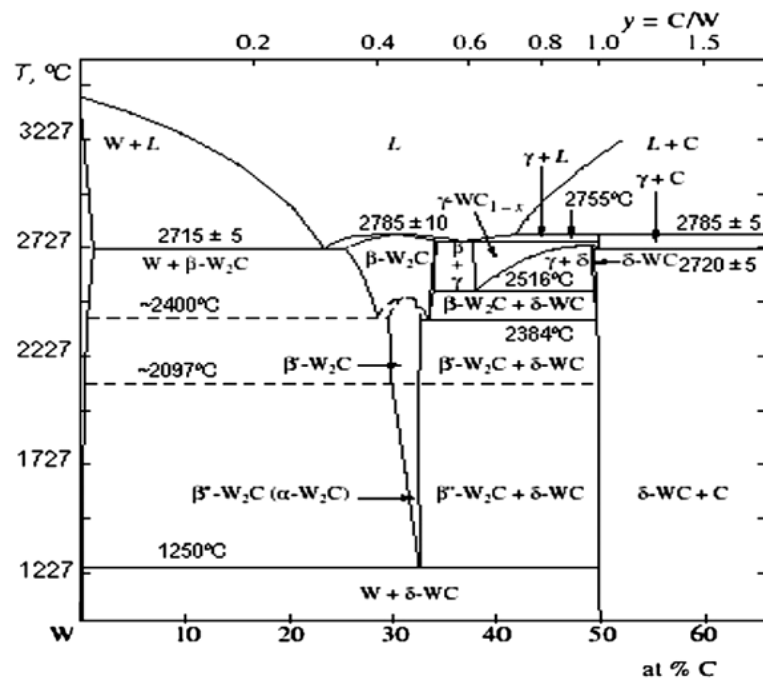


Figure 2.1 W-C phase diagram (Kurlov and Gusev, 2006)

W_2C has hexagonal structure with three modifications: the PbO_2 , Fe_2N , and CdI_2 types, denoted β , β' , and β'' , respectively. These polymorphs are stable at different temperatures. W_2C phase results from the eutectoidal reaction between elemental W and δ -WC at 1250°C and melts congruently at approximately

2785±10°C and forms eutectic melts with the W solid solution at 2215±5°C and with γ -WC_{1-x} at approximately 2755°C, and it exhibits a comparatively wide homogeneity range 25.4-34 at% C at 2715±5°C. The cubic sub-carbide WC_{1-x} (where 1>x>0.5) crystallizing in the NaCl type structure presented γ , and the hexagonal WC denoted δ . This phase is originated from a eutectoidal reaction between β and δ at 2516°C and melts at approximately 2785±5°C.

The technical importance of δ -WC is the only binary phase stable at room temperature and has almost no solid solubility up to 2384°C but may become carbon deficient between this temperature and its incongruent melting point. The δ -WC has a crystal structure of simple hexagonal (space group P6m2) with lattice parameters a = 0.2906 nm and c = 0.28375 nm (c/a ratio of 0.9764). The carbon atoms take the asymmetric position of (1/3, 2/3, 1/2) in the unit cell as shown in Fig. 2.2 and this asymmetric occupation of carbon atoms divides the prismatic planes into two different families of planes with different atom arrangements. These two families of prismatic planes can have a different affinity to carbon because W atoms on each plane have a different number of W–C bonds. The planes with high affinity to carbon grow preferentially in the saturated carbon conditions and disappear finally leaving triangular prism in shape (Kim et al., 2003).

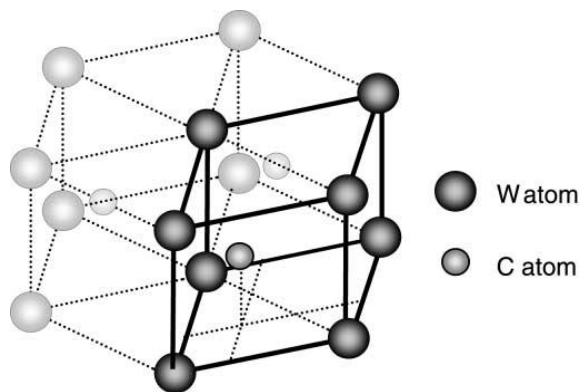


Figure 2.2 The atomic structure of WC crystal (Kim et al., 2003)

The first sintered WC products were produced in 1914 for using in drawing dies and rock drills. Powdered WCs or mixed with Mo₂C were pressed and sintered just below the melting temperature of the pure WC. However, the sintered products were very brittle and unsuccessful in industrial applications (Yao et al., 1998; Yao et al., 1999).

WC hardmetals, as sometimes called cemented WCs, were originated in the USA and in Germany denoted to the electronic incandescent lamp industry. Since the need of a replacement to the expensive diamond dies for being used in the wire-drawing of fine W filaments, manufacturers have been searching for other materials to make the dies. Because of their extreme hardness, WCs are the subject of a potential substantial research and development effort on the part of incandescent lamp industry and their suppliers, for more than two decades (Yao et al., 1998; Yao et al., 1999). The year of 1923 made an important milestone to the invention of WC hardmetals as submitted by Schröter, Germany (Schroter, 1925). In this patent, WC comprising carbon content in the range of 3 – 10 wt.% was mixed with not more than 10 wt.% of metal binders, namely Fe, Ni and Co, and then, the mixture was sintered at the temperature lower than WC melting point, about 1500-1600°C. This patent, then, caused the revolution of metal cutting tool materials and no one could imagine the enormous breakthrough for this material in the tooling industry. When the new tools, made from sintered WC-Co, were first placed in the market in 1927, they caused a sensation in the machine tool industry, by allowing cutting speeds three to five times faster than the best high-speed steel tools in use at that time (Yao et al., 1998; Yao et al., 1999). Few years later, Schwarzkopf discovered that the solid solutions of more than one carbide, particularly TaC, TiC, NbC, VC and Mo₂C, have superior mechanical properties to the individual carbides in cemented hardmetals

(Upadhyaya, 1998; Fernandes and Senos, 2011).

Another important advance in the development of WC hardmetals happened in the late 1960s and early 1970s with the application of coating technique. Hardmetal tools were coated with titanium carbide (TiC), titanium nitride (TiN), titanium carbonitride (TiCN) or alumina (Al_2O_3), which are extremely hard, thus increase the abrasion resistance of hard metals (Yao et al., 1998; Yao et al., 1999; Fernandes and Senos, 2011).

Nowadays, the application of WC hardmetal products has become widely used in various industry sectors including metal cutting, machining of wood, plastics, composites, soft ceramics, chipless forming, mining and construction, structural parts, wear parts, and military components. There has been a continuous expansion in the consumption, from an annual world total of 10 tons in 1930 to about 50,000 tons in 2008. This shows an import role of hardmetals in the world's economy (Schubert et al., 2010).

2.2 Binder phase

The manufacturing process of hardmetals, until now, was based on powder metallurgy (PM) processing including liquid phase sintering. Principle steps of Schröter (Schroter, 1925) invention consist of sintering a mixture of 90 wt.% WC and 10 wt.% binder phase (Fe, Ni, Co) at suitable temperatures at which the binder is liquid and complete consolidation of the compact occurs. The binder phase plays a very important role in sintering of hardmetals. It is responsible for densification through wetting, spreading and formation of agglomerates. The hard phase has a passive role, since the WC particles do not sinter together but are moved by the

binder (Silva et al., 2001). So far, the metallic binder can be a variety of elements, alone or in combination such as Co, Ni, Fe, and Mo or it can also contain other materials, such as stainless steel, superalloys, Ti, etc. In addition, the contents of metal binder have been verified from the original work of Schröter, ranging from 3 to 30 wt.%, even higher (Penrice, 1987; Gille et al., 2000).

2.2.1 Cobalt binder

Since the appearance of WC hardmetals, cobalt has been the optimal choice for the metal binder. Cobalt metal has two allotropic modifications, a close-packed hexagonal (cph) structure, ϵ , stable at temperatures below approximately 400°C, and a face centered cubic (fcc) structure, α , stable at higher temperatures (Upadhyaya, 2001). This metal possesses high hardness, yield stress, toughness and strength. Nowadays, more than 90% of all WC-based hardmetals have been reported using Co as the preferred binder metal with contents ranging from 3 to 30 wt.%. The dominance of Co binder relative to other metal binders is concerned with its superior wettability with WC, higher solubility of WC in Co at sintering temperature and providing excellent mechanical properties to hard metals (Penrice, 1987; Fernandes and Senos, 2011).

The understanding of the phase diagram of cemented carbides is an important tool to predict *phase composition* after sintering step and to select the *adequate sintering* conditions. The vertical section of the W-C-Co phase diagram calculated at 10 wt.% Co is shown in Fig. 2.3 (Guillermat, 1989a). The best properties of WC-Co system have been obtained within the two phase region, fcc-Co and WC phase. The points denoted as a and b in Fig. 2.3 define, respectively,

minimum and maximum carbon contents of alloys which are in two-phase state of fcc Co and WC just after the equilibrium solidification. Due to the important role of WC-Co hard metals, several investigations concerning the W-C-Co system have been carried out over the last century (Pollock and Stadelmaier, 1970; Guillermet, 1989a; Markström et al., 2005). Some physical and mechanical properties of WC-Co obtained from those works are listed in Table 2.1.

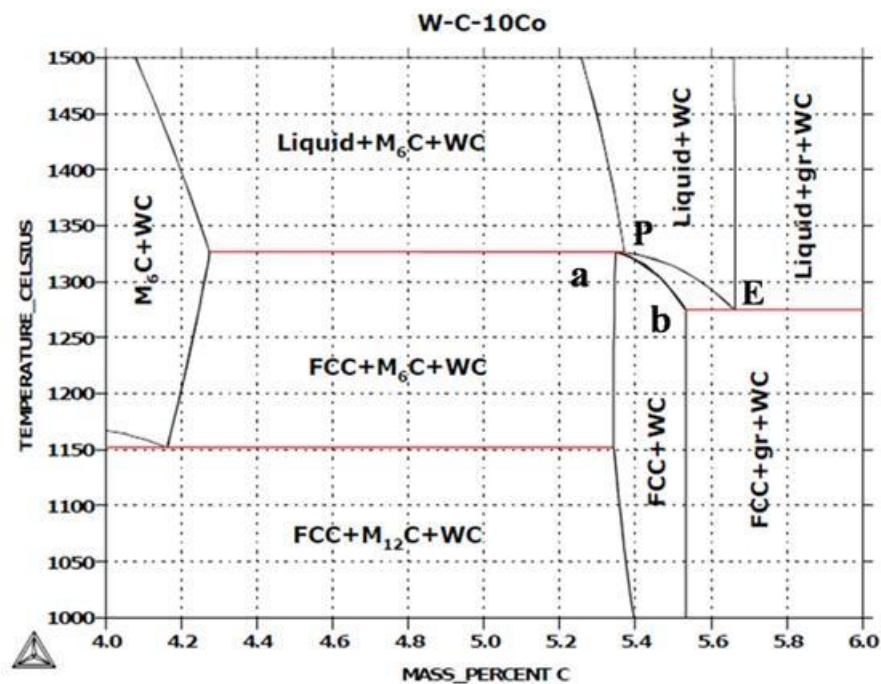


Figure 2.3 Vertical section of W-C-Co calculated at 10 wt.% Co: M_6C (η -phase, Co_3W_3C), FCC (γ -Co), gr (graphite), P (peritectic point), E (eutectic point) (Guillermet, 1989a)

Table 2.1 Physical and mechanical properties of some WC-Co hardmetals

Nominal composition	Average grain size (μm)	Density (g/cm^3)	Hardness (HV)	Fracture toughness ($\text{MPa}\cdot\text{m}^{1/2}$)	Kc (N/mm)	Reference
94WC+6Co	0.1	14.83	2280	-	370	
90WC+10Co	0.1	14.46	2043	-	530	Gille et al., 2000
88WC+12Co	0.1	14.30	1910	-	570	
85WC+15Co	0.1	13.95	1700	-	725	
85WC+15Co	0.258	14.53	1992	11.9	-	Kim et al., 2004
90WC+10Co	0.38	14.79	1756	11.6	-	Kim et al., 2007
WC+2.9Co	0.94	14.51	2014	6.5	-	
WC+12Co	<1	-	1748	11.4	-	Deorsola et al., 2010

Besides the aim to get two-phase state of WC-Co hard metals after sintering, the tendency to produce fine and ultrafine or nano microstructure of WC-Co hardmetals arises from the understanding that the mechanical properties such as hardness and wear resistance increase with the decrease of WC grain size. To fulfill the requirements of the hardmetal industry and the trend toward finer grain size tools, several studies have been done (Gille et al., 2000; Kim et al., 2004; Kim et al., 2007; Deorsola et al., 2010).

2.2.2 Nickel binder

Ni has been proposed in many researches as the binder phase to WC-based hardmetals, mainly as a substitute for Co during periods of Co scarcity. Ni retains its fcc structure at all temperatures below its melting point and a similarly lattice parameter of fcc Ni compared to fcc Co. The melting point of Ni at 1453°C is appreciably lower than Co at 1495°C, however it is necessary to use increased

sintering time and temperature to gain satisfactory densification (Penrice, 1987; Fernandes and Senos, 2011). Vertical section of W-C-Ni phase diagram calculated at 10 wt.% Ni is shown in Fig. 2.4 (Guillermet, 1989b). Comparing with the corresponding section of W-C-Co in Fig. 2.3, the width of two-phase state region remain essentially similar, however the range of favorable C contents moves backwards to lower value as comparison with the stoichiometric composition. In addition, the change from W-C-Co to W-C-Ni involves an appreciable increase in the equilibrium temperature of eutectic (E) and peritectic (P) points (Figs. 2.3 and 2.4) (Raghavan, 2007).

The partial or complete replacement of Co by Ni leads to a decrease of hardness of hardmetals. The decrease of hardness is probably the principal reason why Ni has not been accepted widely to replace Co in WC hard metal industry, exceptionally in very significant quantities of wear applications where require higher corrosion and erosion resistance or higher oxidation (Penrice, 1987; Tracey, 1992; Voitovich et al., 1996). In some cases, mixtures of Co-Ni were used as the binder to improve toughness but not significantly reducing hardness for economic purpose or some applications such as in mining and hot rolling equipments (Voitovich et al., 1996; Zhang and Sun, 1996; Aristizabal et al., 2012).

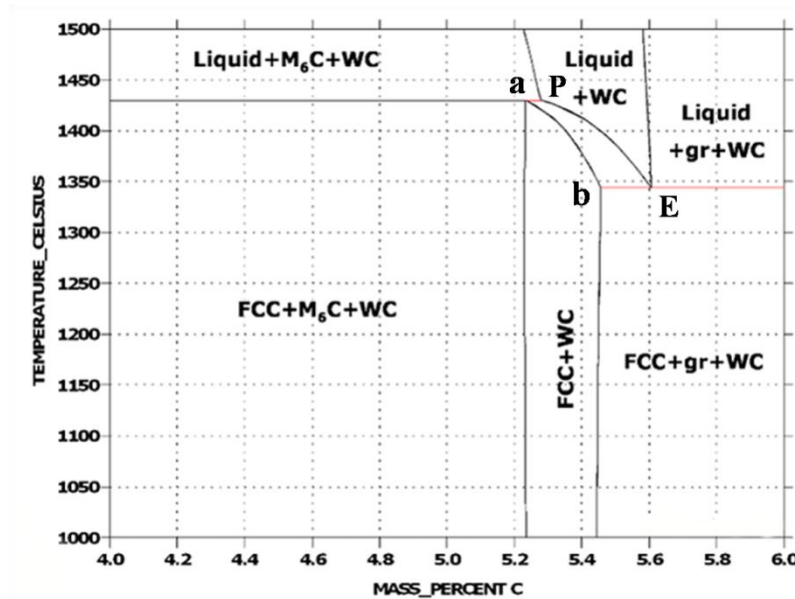


Figure 2.4 Vertical section of W-C-Ni calculated at 10 wt.% Ni: M_6C (η -phase, Ni_3W_3C), FCC (γ -Ni), gr (graphite), P (peritectic point), E (eutectic point) (Guillermet, 1989b)

2.2.3 Iron binder

Iron is a soft metal that can dissolve a small amount of C (0.021 wt.%) up to 910°C with a magnetic bcc crystal structure, called α -Fe (ferrite). At the higher temperature, up to 1400°C , and in the presence of higher C contents, α -Fe undergoes a phase transition from bcc to fcc crystal structure, also called γ -Fe (austenite). This phase is metallic and non-magnetic and dissolve considerably more C, 2.04 wt.% at 1146°C (Fernandes and Senos, 2011).

The W-C-Fe system has been subjected to several experiments and theoretical investigation over the years Bergström, 1977; Gustafson, 1988; Guillermet, 1989b. A vertical section of W-C-Fe phase diagram calculated at 10 wt.% Fe can be seen in Fig. 2.5 (Guillermet, 1989b). The two-phase state region moves to higher content of C. Fe forms a ternary eutectic melt at only 1143°C and it

also a possible replacement for Co (Jia et al., 1998). However, complete substitute of Co by Fe in WC-based hardmetal did not hold much promise. Fe, unlike Co, is a carbide former, thus, a C-rich composition is needed and even to control material within two-phase state is difficult (Penrice, 1987).

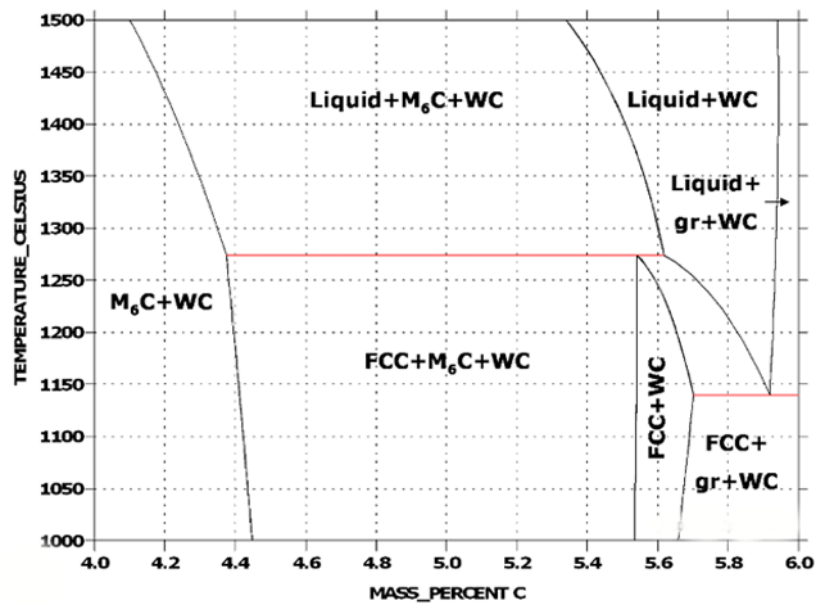


Figure 2.5 Vertical section of W-C-Ni calculated at 10 wt.% Fe (Guillermat, 1989b)

2.2.4 Ni-Fe and Co-Ni-Fe binders

The complete substitution of Ni-Fe binder to Co in WC-10 wt.% Co has been reported having better properties in comparison with the substitution by either Fe or Ni alone (Upadhyaya and Bhaumik, 1988). This study also shows that the grain size of WC increased with increasing of Ni content in the binder but resulting in a decrease of oxidation resistance. In other study, the hardness of WC-(Fe,Ni) with Fe-rich binder depends on the C contents and lower than WC-Co one (Uhrenius et al., 1997). The study also shows that the Ni-rich Ni-Fe or Ni-Fe-Co binders have no tendency to increase hardness for composition close to or within the two-phase region of WC and fcc metal. In general, C content plays an important role in

controlling phase and final density, and consequently, influences on mechanical properties of WC-(Fe,Ni,C) hardmetals (Viswanadham and Lindquist, 1987; González et al., 1995; Uhrenius et al., 1997). Controlling the phase formation of WC-(Fe,Ni,C) by heat treatment has been also carried out to get higher mechanical properties of WC-(Fe,22Ni,C) (Viswanadham and Lindquist, 1987). The study also suggested that the hardness and fracture toughness improved at the suitable content of C after quenching in liquid nitrogen.

Partially replacement of Co binder by a Co-rich binder (60Co-20Ni-20Fe) and a Fe-rich binder (75Fe-15Ni-10Co) have been done in WC-Co hardmetals with 2.5 μm of WC grain size (Gille et al., 2000). The results show that the hardmetals with Fe-rich binder are higher in hardness but lower in toughness in comparison to Co-rich binder hardmetals.

2.2.5 Fe-Cr-Ni binders and stainless steel binder

Different compositions of Fe-Cr-Ni have been used as the replace binder to Co in WC-10Co hardmetals using magnetron sputtering method to coat WC powders and sintering in a vacuum furnace (Fernandes et al., 2007; Fernandes et al., 2009a). The thermal reactivity between WC and Fe/Cr/Ni was investigated (Fernandes et al., 2009a). The results show that no η -phase occurs for WC-10Fe after sintering at 1400°C and the substitution of half percent of the Fe content by Ni stabilized the austenite γ -Fe. The introduction of Cr in the binder induced the formation of Cr_2C and limited the formation of η -phase. Decreasing Cr content leads to the formation of η -phase. The addition of graphite has enabled to reduce η -phase formation in WC-Fe/Ni/Cr hardmetals as well (Fernandes et al., 2007; Fernandes et al., 2009a).

The use of AISI304 stainless steel has been also proposed as binder to replace Co (Fernandes et al., 2003a; Fernandes et al., 2006). Particle surface investigation revealed that a high uniformity of the coating distribution on WC particles was attained by sputtering technique, enabling to complete surface coverage at low binder content (≥ 1 wt.%) (Fernandes et al., 2006). The sputtering technique is shown to be efficient in promoting densification of hardmetals, which has been attributed to the high uniformity of coated powder. High densities (of approximately 95 %) were obtained at a relatively low sintering temperature (1325°C) with only 6 wt.% of binder phase (Fernandes et al., 2003a).

2.3 η - Phase

Decarburization of WC or deficiency of C comparing to stoichiometric leads to the formation of ternary compounds of W, Co and C, called η -phase that exists in two types: M_6C and $M_{12}C$ ($M=W$ and Co or Fe). $M_{12}C$ phase is substantially constant composition. On the other hand, M_6C can vary within the range of $M_{3.2}W_{2.8}C$ and M_2W_4C . The M_6C type of η -phase is in equilibrium with the liquid phase and can nucleate and grow during the sintering process. The $M_{12}C$ type is formed in the solid state (during cooling) with small grains distributed throughout the matrix and is therefore effectively less embrittling (Yao et al., 1998; Yao et al., 1999) than M_6C . However, M_6C was reported to be the most high-temperature stable carbide (Pollock and Stadelmaier, 1970).

The M_6C carbide, which has many isomorphs among ternary carbides, contains at least two types of metal atoms. Its formation is favoured by the combination of one weak and other strong carbide formers, e.g. Fe and W

(Bergström, 1977). All the examined η -phases ($\text{Fe}_3\text{W}_3\text{C}$, $\text{Fe}_6\text{W}_6\text{C}$, $\text{Co}_3\text{W}_3\text{C}$, $\text{Co}_6\text{W}_6\text{C}$) adopt the cubic symmetry with the space group $\text{Fd}\bar{3}\text{m}$ and $Z = 16$ (for $\text{Fe}_3\text{W}_3\text{C}$ and $\text{Co}_3\text{W}_3\text{C}$) and $Z = 8$ (for $\text{Fe}_6\text{W}_6\text{C}$ and $\text{Co}_6\text{W}_6\text{C}$), (Z : the number of C atoms). The M_6C carbide has a fcc structure ($\text{cF}112$) containing 96 atoms per unit cell. The W atoms occupy the $48f$ sites; Fe and Co are placed in two non-equivalent $32e$ and $16d$ sites, where as C is located in the $16c$. The only difference between $\text{M}_3\text{W}_3\text{C}$ and $\text{M}_6\text{W}_6\text{C}$ is that these phase contain 16 and 8 C atoms (per cell), respectively (Suetin et al., 2009, Ramnath and Jayaraman, 1987).

η - phase formation moves to low C contents in the phase diagram. Fig. 2.6 shows the ternary diagrams of W-Co-C calculated at 1000°C and 1400°C (Pollock and Stadelmaier, 1970). While the homogeneity range of M_{12} was found to remain small, M_6C spread out to include $\text{Co}_3\text{W}_3\text{C}$ and $\text{Co}_2\text{W}_4\text{C}$ at 1400°C and narrowed back down to a small range around $\text{Co}_2\text{W}_4\text{C}$ at 1000°C . Their evaluation of the η - phase in W-Co-C system based on XRD patterns of as-cast alloys revealed two η - phases, $\text{Co}_6\text{W}_6\text{C}$ and $\text{Co}_2\text{W}_4\text{C}$ with lattice constants near 10.90 and 11.20 Å, respectively.

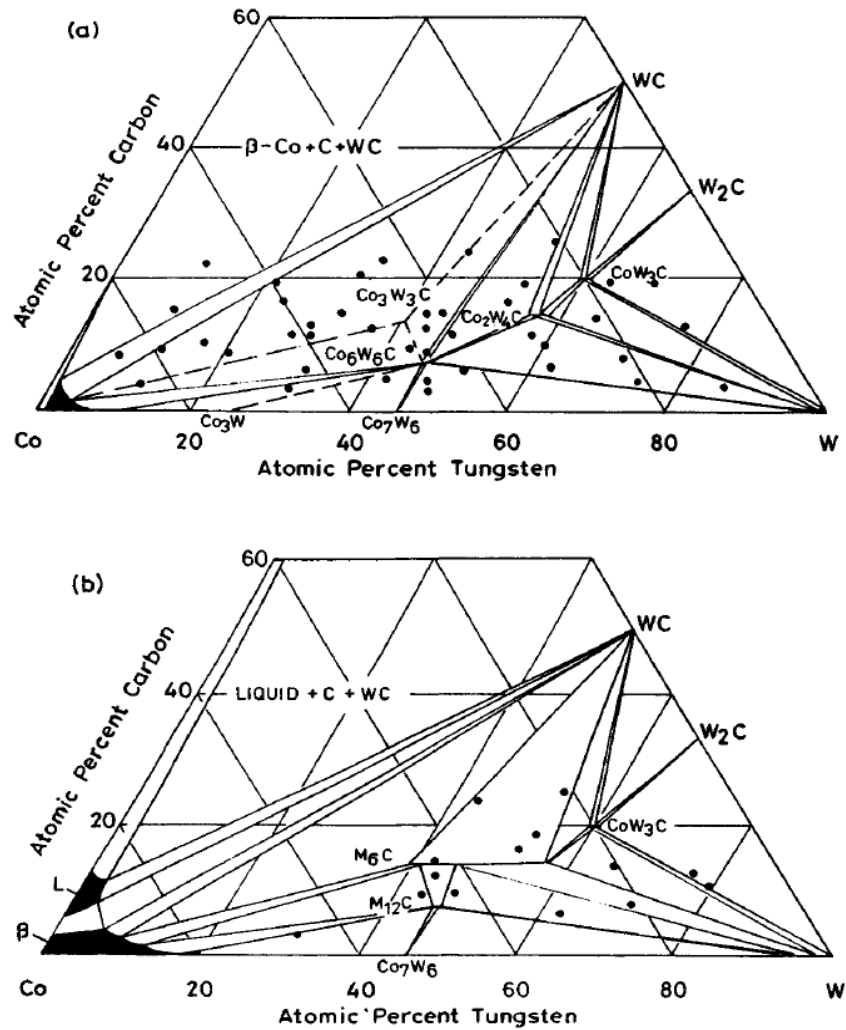


Figure 2.6 W-Co-C isothermal sections: a) at 1000°C and b) 1400°C
(Pollock and Stadelmaier, 1970)

The ideal structure of M_6C is quite complicated and consists of eight regular octahedral of W atoms centered in a diamond cubic lattice and eight regular tetrahedral of Fe (or Co) atoms centered in the second diamond cubic lattice that interpenetrates the first through the $1/2, 1/2, 1/2$ unit cell translation. Sixteen additional Fe (or Co) atoms are tetrahedrally coordinated around the Fe (or Co) tetrahedral and sixteen C atoms surround the W octahedral in tetrahedral coordination (Suetin et al., 2009). The model crystal structure of Fe_3W_3C is shown in Fig. 2.7 (Fernandes, 2008).

η -phase is an undesired phase in microstructure of sintered products because it results in degradation of mechanical properties and cutting performance (Yao et al., 1998). This brittle phase was attributed to the decrease of fracture toughness of hardmetals (González et al., 1995; Uhrenius et al., 1997; Upadhyaya, 1998; Upadhyaya et al., 2001). The transverse rupture strength was achieved highest value without the presence of η -phase in WC-6Co (Upadhyaya et al., 2001).

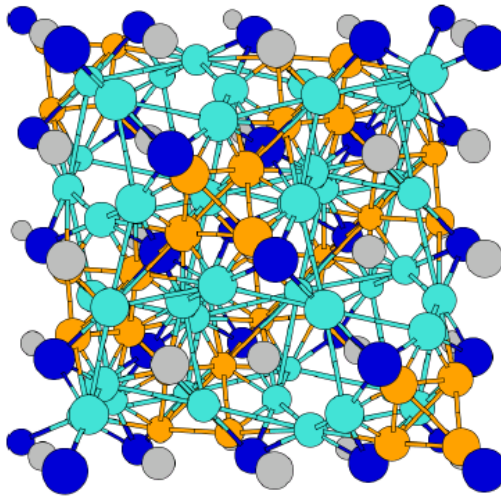


Figure 2.7. Crystal structure of $\text{Fe}_3\text{W}_3\text{C}$; ● Carbon ● Tungsten ● Iron
(Fernandes, 2008)

2.4 Graphite

Graphite, C_{gr} , is an allotrope of C. There are two forms of C_{gr} in nature: $\alpha\text{-C}_{\text{gr}}$ with hexagonal structure and $\beta\text{-C}_{\text{gr}}$ having rhombohedra structure. Most of C_{gr} is $\alpha\text{-C}_{\text{gr}}$ and it possesses a layer structure in which each C is directly bound to three other C atoms at a distance of 1.415Å . The layer planes are stacked parallel to each other at the distance of 3.354Å . And, the layers of atoms are arranged in an ABABAB... repeat fashion. The only difference of the β -form (rhombohedral) is the layers in the arrangement of ABCABCABC... although the C-C distances and the